THE JOURNAL OF BIOLOGICAL CHEMISTRY
Vol. 276, No. 36, Issue of September 7, pp. 34348–34354, 2001
Printed in U.S.A.

Motor Function and Regulation of Myosin X*

Received for publication, May 25, 2001, and in revised form, July 12, 2001
Published, JBC Papers in Press, July 16, 2001, DOI 10.1074/jbc.M104785200

Kazuaki Homma, Junya Saito, Reiko Ikebe, and Mitsuo Ikebe‡

From the Department of Physiology, University of Massachusetts Medical School, Worcester, Massachusetts 01655-0127

Myosin X is a member of the diverse myosin superfamily that is ubiquitously expressed in various mammalian tissues. Although its association with actin in cells has been shown, little is known about its biochemical and mechanoenzymatic function at the molecular level. We expressed bovine myosin X containing the entire head, neck, and coiled-coil domain and purified bovine myosin X in Sf9 cells. The Mg^{2+}-ATPase activity of myosin X was significantly activated by actin with low K_{ATP}. The actin-activated ATPase activity was reduced at Ca^{2+} concentrations above *p*Ca 5 in which 1 mol of calmodulin light chain dissociates from the heavy chain. Myosin X translocates F-actin filaments with the velocity of 0.3 μm/s with the direction toward the barbed end. The actin translocating activity was inhibited at concentrations of Ca^{2+} at *p*Ca 6 in which no calmodulin dissociation takes place, suggesting that the calmodulin dissociation is not required for the inhibition of the motility. Unlike class V myosin, which shows a high affinity for F-actin in the presence of ATP, the K_{actin} of the myosin X ATPase was much higher than that of myosin V. Consistently nearly all actin dissociated from myosin X in the presence of ATP. ADP did not significantly inhibit the actin-activated ATPase activity of myosin X, suggesting that the ADP release step is not rate-limiting. These results suggest that myosin X is a nonprocessive motor. Consistently myosin X failed to support the actin translocation at low density in an *in vitro* motility assay where myosin V, a processive motor, supports the actin filament movement.

Myosins are actin-based motor proteins that play a role in diverse cellular movement. Myosin is composed of a motor domain containing an ATP and actin binding region, a neck domain that interacts with specific light chains or calmodulin, and a tail domain that serves to anchor myosin to a specific cellular target. In the last decade, a number of different types of myosins have been discovered by molecular cloning, and based upon their primary structure of the motor domain they are classified in at least 18 classes (1–6).

Myosin X is a newly found myosin from bovine, human (7), and mouse (8), and it is expressed ubiquitously in various mammalian tissues. Based upon the deduced amino acid sequence, it is predicted that myosin X consists of a motor domain, three IQ motifs that function as light chain binding sites, a coiled-coil domain, and a tail domain. Because of the presence of a coiled-coil domain, it has been thought that myosin X is a two-headed myosin. There are three pleckstrin homology domains, one myosin tail homology domain, and one FERM (4.1/Ezrin/Radixin/Moesin) domain in each heavy chain. Although the actual function of these domains is not known, they could play a role in interactions with membrane phospholipids or other proteins that create an anchoring structure.

By immunocytochemistry, it was found (7) that myosin X is present at the edge of lamellipodia, membrane ruffles, and the tip of filopodial actin bundles in cultured cells, suggesting that myosin X plays a role in regions where actin is in dynamic reorganization. The localization of myosin X with the actin structure in cells along with the structural features present in myosin X that are conserved among various myosins suggests that myosin X has an actin-based motor activity. However, nothing is known about the motor function of myosin X at a molecular level.

There are two aspects underlying the diverse biological function of the myosin superfamily members. One is their unique tail structure, and it is anticipated that each unique tail determines the cellular target molecules thus distributing each myosin for its proper motile processes. The other is the characteristic of myosins in terms of their motor function and regulation. It becomes evident that the motor function among various members of the unconventional myosin subfamily varies uniquely from one to another; this variation is thought to be critical for specific physiological roles in diverse cellular motile processes. Myosin V is a processive motor that can move in large steps approximating the 36-nm pseudo-repeat of the actin filament (9, 10). These characteristics are quite important to understand the cellular function of myosin V because the processive nature with long step size is suitable for motors involved in cargo movement in cells. Another amazing finding is that myosin VI moves the actin filament with the barbed end leading, indicating that myosin VI moves toward the pointed end, whereas all other characterized myosin motors move toward the barbed end (11). Because actin structure in cells has polarity, the directionality of the movement is quite important for the physiological relevance of the motor protein.

Although it was originally proposed that a unique large insertion of 53 residues between the converter domain and IQ domain of myosin VI plays a key role in the reverse-directed movement of myosin VI, recent results have suggested that this is not the case and that the motor domain itself determines the directionality of myosin VI (12). This raises the possibility that other unconventional myosins may show reverse directionality.

The role of the IQ motif in unconventional myosins is best studied in myosin I (13–17) and V (18). These myosins contain calmodulin as their light chain that associates with the heavy chain at the IQ region. The ATPase activities of these myosins are regulated by Ca^{2+}-induced calmodulin dissociation from the myosin heavy chain. On the other hand, motility activities are completely abolished at *p*Ca 6 in which calmodulin does not dissociate from myosin heavy chain, suggesting that Ca^{2+}-

* This work was supported by National Institutes of Health Grants AR 41653, HL 60381, and GM 55834. The costs of publication of this article were defrayed in part by the payment of page charges. This article must therefore be hereby marked "*advertisement*" in accordance with 18 U.S.C. Section 1734 solely to indicate this fact.

‡ To whom correspondence should be addressed: Dept. of Physiology, University of Massachusetts Medical School, 55 Lake Ave. North, Worcester, MA 01655-0127. Tel.: 508-856-1954; Fax: 508-856-4600; E-mail: mitsuo.ikebe@umassmed.edu.

induced conformational change of calmodulin, but not physical dissociation of calmodulin from the heavy chain, is critical for the regulation of motility activity of these myosins. Although nothing is known about the regulation of myosin X, a similar mechanism might be operating because it contains three IQ motifs at its neck domain.

The aim of this study was to clarify the motor function and regulation of mammalian myosin X at the molecular level. To achieve this, we expressed myosin X by using a baculovirus expression system because the myosin X expression level in tissues is limited. Our results indicated that myosin X is a plus end-directed nonprocessive motor whose motility activity is inhibited at high Ca^{2+}.

EXPERIMENTAL PROCEDURES

Materials—Restriction enzymes and modifying enzymes were purchased from New England Biolabs (Beverly, MA). Actin was prepared from rabbit skeletal muscle acetone powder according to Spudich and Watt (19). Recombinant calmodulin from *Xenopus* oocytes (20) was expressed in *Escherichia coli* as described previously (21). Smooth muscle myosin and myosin light chain kinase were prepared as described previously (22, 23). Myosin V heavy meromyosin was prepared as described previously (18). Smooth muscle myosin was phosphorylated with 15 μg/ml myosin light chain kinase in the presence of 10 μg/ml calmodulin, 2 mM ATP, 2 mM $MgCl_2$, 50 mM KCl, and 30 mM Tris-HCl (pH 7.5) at 25 °C for 15 min in the presence of 1 μM microcystin.

Molecular Cloning of the Bovine Myosin X Construct—Three cDNA clones of bovine myosin X, *i.e.* clones 17 (nucleotides 1–1564), 27 (nucleotides 976–2653), and 5-2-1 (nucleotides 2030–7769), were kindly provided by Dr. D. P. Corey (Harvard University). An *Nhe*I site and an *Eco*RI site were created at the 5′-side of the initiation site and nucleotide 1240 of clone 27, respectively. An *Eco*RI site and an *Xba*I site were created at nucleotides 1240 and 2517 of clone 17, respectively. Two *Xba*I sites were also created at nucleotides 2517 and 3138 of clone 5-2-1, respectively. The clone 27 was then digested with *Nhe*I/*Eco*RI, and the fragment was subcloned into pFastBac baculovirus transfer vector containing a hexahistidine tag sequence at the 3′-end of the polylinker region. Clone 17 was digested with *Eco*RI/*Xba*I, and the 1.3-kilobase fragment was introduced into pFastBac/clone 27. Finally an *Xba*I fragment (0.6 kilobase) excised from clone 5-2-1 was inserted into the above vector. This construct (M10CC) contains the entire motor domain, neck domain, and coiled-coil domain with a hexahistidine tag at the C-terminal end.

Preparation of Recombinant Myosin X—To express recombinant myosin X, 200 ml of Sf9 cells (about 1×10^9) were co-infected with two separate viruses expressing the myosin X heavy chain and calmodulin, respectively. The cells were cultured at 28 °C in 175-cm^2 flasks and harvested after 3 days. Cells were lysed with sonication in 20 ml of Lysis Buffer (0.1 M NaCl, 30 mM Tris-HCl (pH 7.5), 2 mM $MgCl_2$, 0.2 mM EGTA, 10 mM β-mercaptoethanol, 1 mM phenylmethanesulfonyl fluoride, 0.01 mg/ml leupeptin, 0.1 mg/ml trypsin inhibitor, and 1 mM ATP). After centrifugation at 140,000 $\times$ *g* for 20 min, the supernatant was mixed with 0.3 ml of nickel-nitrilotriacetic acid (Ni-NTA) agarose (Qiagen, Hilden, Germany) in a 50-ml conical tube on a rotating wheel for 20 min at 4 °C. The resin suspension was then loaded on a column (1×10 cm) and was washed with a 10-fold volume of buffer B (0.3 M KCl, 10 mM imidazole (pH 7.5), 0.1 mM EGTA, and 10 mM β-mercaptoethanol, and 0.01 mg/ml leupeptin). Myosin X was eluted with buffer B plus 0.2 M imidazole.

After SDS-PAGE[1] analysis, fractions containing myosin X were pooled and dialyzed against 30 mM KCl, 20 mM MOPS (pH 7.0), 0.1 mM EGTA, and 1 mM dithiothreitol. The purified myosin X was stored on ice and used within 2 days.

Gel Electrophoresis and ATPase Assay—SDS-polyacrylamide gel electrophoresis was carried out on a 7.5–20% polyacrylamide gradient slab gel using the discontinuous buffer system of Laemmli (24). The molecular mass markers used were smooth muscle myosin heavy chain (204 kDa), β-galactosidase (116 kDa), phosphorylase *b* (97.4 kDa), bovine serum albumin (66 kDa), ovalbumin (45 kDa), carbonic anhydrase (29 kDa), myosin regulatory light chain (20 kDa), and α-lactalbumin (14.2 kDa). The amount of the myosin X heavy chain and calmodulin was determined by densitometry as described previously (14). The steady state ATPase activity was determined by measuring liberated $^{32}P_i$ at 25 °C as described previously (22). The ATPase activity was also measured in the presence of an ATP regeneration system, 20 units/ml pyruvate kinase, and 3 mM phosphoenolpyruvate. The liberated pyruvate was determined as described previously (25).

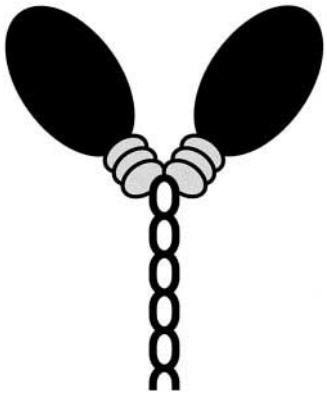

FIG. 1. **Schematic drawing of the myosin X construct M10CC.** The motor domain of myosin X is indicated by the *filled black ovals*. Calmodulin light chains are indicated by *dotted shapes*. The coiled-coil domain is indicated by a *chain*.

In Vitro Motility Assay—The *in vitro* motility assay was performed as described previously (26). Myosin X was attached to the coverslip. Actin filament velocity was calculated from the movement distance and the elapsed time in successive snapshots. Student's *t* test was used for statistical comparison of mean values. A value of $p < 0.01$ was considered to be significant.

Preparation of the Dual Labeled F-actin—F-actin (1.3 mg/ml) was first labeled with a 5 molar excess of tetramethylrhodamine-5-(or -6-)-maleimide (Molecular Probes, Eugene, OR) in the presence of 8 μM phalloidin, 25 mM KCl, 5 mM $MgCl_2$, 1 mM EGTA, and 25 mM imidazole (pH 7.5) (buffer A) in the dark for 40 min at 4 °C. After the reaction was stopped by adding 10 mM dithiothreitol, the fluorescently labeled F-actin was obtained by centrifugation (250,000 $\times$ *g* for 10 min). The pellet was homogenized with buffer A with 5 mM dithiothreitol and then precipitated again (250,000 $\times$ *g* for 10 min) to wash away the residual dye. The homogenate was diluted with the same buffer (F-actin concentration should be ~0.03 mg/ml) and subjected to sonication to make the minus end cap. The fragmentation of the fluorescently labeled F-actin was confirmed under a fluorescence microscope. 0.1–1 μM G-actin was added to the fragmented fluorescently labeled F-actin (2–15 μg/ml) in 25 mM KCl, 5 mM $MgCl_2$, 1 mM EGTA, 25 mM imidazole (pH 7.5), and 10 units/ml fluorescein phalloidin (Molecular Probes). The elongation of the actin filament was carried out overnight in the dark at 4 °C.

Actin Co-sedimentation Assay—The binding of calmodulin to M10CC heavy chain was determined by actin co-sedimentation assay. M10CC was incubated in buffer containing 20 mM MOPS (pH 7.0), 10 mM KCl, 2 mM $MgCl_2$, 1 mM $CaCl_2$, 0.025 mg/ml F-actin, and various concentrations of EGTA at 25 °C for 15 min. The sample was ultracentrifuged at 100,000 $\times$ *g* for 30 min, and the pellets were analyzed by SDS-polyacrylamide gel electrophoresis. The amount of the co-sedimented M10CC heavy chain and calmodulin were determined by densitometry as described previously (14).

RESULTS

Expression and Purification of Mammalian Myosin X—The bovine myosin X construct was produced and expressed in Sf9 insect cells. The construct (M10CC) contains the entire coiled-coil domain in addition to the complete head domain with a C-terminal hexahistidine tag to aid in purification (Fig. 1). The cells were co-infected with an appropriate ratio of myosin X-expressing virus and calmodulin-expressing virus. The functional myosin X was only obtained with co-infection of calmodulin virus in contrast to myosin V in which functional protein can be obtained without calmodulin co-infection (27). The myosin X-enriched fraction was applied to a nickel-agarose affinity column using the hexahistidine tag to completely purify the expressed myosin X (M10CC) (Fig. 2).

Fig. 2 shows SDS-PAGE of the purified myosin X. The puri-

[1] The abbreviations used are: PAGE, polyacrylamide gel electrophoresis; CLP, calmodulin-like protein; MOPS, 4-morpholinepropanesulfonic acid.

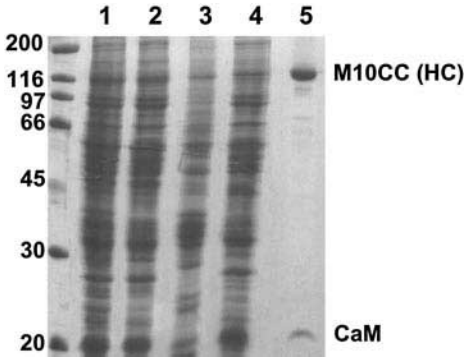

FIG. 2. **Expression and purification of M10CC.** The sample of each purification step was examined by SDS-PAGE and stained with Coomassie Brilliant Blue. *Lane 1*, total cell lysate homogenized with buffer containing 30 mM Tris-HCl (pH 7.5), 0.1 M NaCl, 10 mM β-mercaptoethanol, 0.2 mM EGTA, 2 mM $MgCl_2$, 1 mM ATP, 1 mM phenylmethanesulfonyl fluoride, 0.1 mg/ml trypsin inhibitor, and 0.01 mg/ml leupeptin; *lane 2*, 100,000 × *g* supernatant; *lane 3*, 100,000 × *g* pellets; *lane 4*, unbound fraction after loading the supernatant onto a nickel-nitrilotriacetic acid-agarose column; *lane 5*, eluate with 200 mM imidazole (pH 7.5), 0.3 M KCl, 0.2 mM EGTA, and 10 mM β-mercaptoethanol. *HC*, heavy chain; *CaM*, calmodulin.

fied M10CC construct was composed of a high molecular mass band and a low molecular mass band and was free from 200-kDa Sf9 conventional myosin and actin. The high molecular mass band (110 kDa) was consistent with the calculated molecular mass of M10CC and was recognized by anti-His antibodies (Santa Cruz Biochemicals, Santa Cruz, CA) indicating that the high molecular mass band is the expressed myosin X heavy chains (not shown). The small subunits showed a mobility shift with a change in $[Ca^{2+}]$ that is characteristic of calmodulin, suggesting that the small subunits are indeed calmodulin (not shown). The identification of the small subunit was also confirmed using anti-calmodulin antibodies (not shown). The stoichiometry of calmodulin *versus* M10CC heavy chain was determined by densitometry to be 2.8 ± 0.3, consistent with the three IQ motifs in M10CC construct.

Actin-activated ATPase Activity of Myosin X—The Mg^{2+}-ATPase activity of myosin X was markedly activated by actin. Fig. 3 shows the actin concentration dependence of the actin-activated ATPase activity of myosin X. The actin concentration required for the saturation of the activation was much higher than that of myosin V (18, 27, 28) but rather similar to that of conventional myosin. The curve fit with an equation of $v = V_m[\text{actin}]/(K_{\text{actin}} + [\text{actin}])$ gave a K_{actin} of 28 μM. The result suggests that the predominant steady state intermediate of the myosin X ATPase reaction is a weak actin binding state.

Fig. 4 shows the actin-activated ATPase activity as a function of ATP concentration. The ATP dependence shows a single saturation curve, and a K_{ATP} of 3.4 μM was obtained from the best curve fit analysis, suggesting a high affinity of myosin X for ATP. It has been shown that the actin-activated ATPase activity of myosin V is markedly attenuated with reaction time, and this is due to the inhibition by ADP liberated during the ATPase reaction. This suggests a high affinity of myosin V for ADP. Fig. 5 shows the time course of the actin-activated ATPase reaction of myosin X. In contrast to myosin V, the ATPase activity in the absence of the ATP regeneration system was not significantly changed with time, although the activity was slightly decreased at a prolonged time. The activity in the absence of the ATP regeneration system at the early time was nearly identical to that in the presence of the ATP regeneration system. The result indicates that actomyosin X ATPase activity is not significantly inhibited by ADP. To further confirm this notion, the ATPase activity was measured as a function of ADP (Fig. 6). ADP did not strongly inhibit the ATPase activity, and

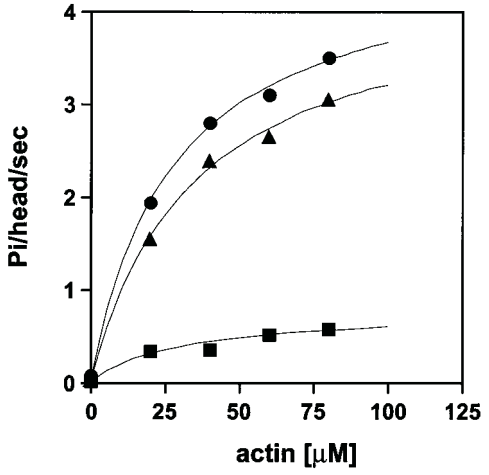

FIG. 3. **Actin concentration dependence of the Mg^{2+}-ATPase activity of M10CC.** The actin-activated ATPase activity of M10CC was measured as a function of actin concentration in either 1 mM EGTA ( ), 100 μM Ca^{2+} (■), or 100 μM Ca^{2+} + 0.2 mg/ml calmodulin (▲). Actin-activated ATPase activity of M10CC (42 nM) was assayed in buffer containing 20 mM MOPS (pH 7.0), 10 mM KCl, 2 mM $MgCl_2$, 2 mM ATP, and 1 mM EGTA or *p*Ca 4 at 25 °C. *Solid lines* are the calculated lines based upon the equation $v = V_m[\text{actin}]/(K_{\text{actin}} + [\text{actin}])$. According to the analysis, V_m and K_{actin} were 4.7 s^{-1} and 28 μM in the presence of EGTA, 0.77 s^{-1} and 32 μM in *p*Ca 4, and 4.3 s^{-1} and 35 μM in *p*Ca 4 + 0.2 mg/ml calmodulin, respectively.

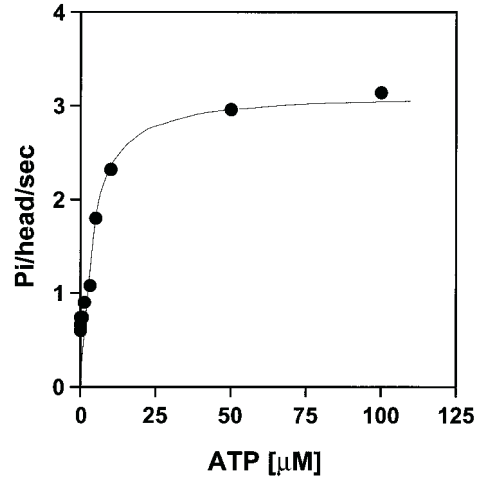

FIG. 4. **ATP dependence of the actin-activated Mg^{2+}-ATPase activity of M10CC.** The ATPase activity was measured as described in the legend for Fig. 3 (1 mM EGTA), except 50 μM actin and various ATP concentrations were used. A *solid line* is the calculated line based upon the equation $v = (V_m[\text{ATP}]/K_{\text{ATP}} + [\text{ATP}])$. According to the analysis, V_m and K_{ATP} were 3.1 s^{-1} and 3.4 μM, respectively.

the curve fit analysis with the equation of $v = V_m[\text{ATP}]/(K_{\text{ATP}}(1 + [\text{ADP}]/K_{\text{ADP}}) + [\text{ATP}])$ yielded a K_{ADP} of 6.4 μM.

The actin-activated ATPase activity was measured as a function of free Ca^{2+} because other calmodulin-bound unconventional myosins such as myosin I and myosin V show Ca^{2+} dependence on their actin-activated ATPase activity (15–18, 29, 30). The activity markedly decreased with an increase in Ca^{2+} from *p*Ca 6 to *p*Ca 5 (Fig. 7). The decrease in the activity above *p*Ca 5 was rescued by the addition of exogenous calmodulin, suggesting that the decrease in the activity at this range of Ca^{2+} is because of the dissociation of calmodulin from the myosin X heavy chain. The low ATPase activity in high Ca^{2+} is because of the decrease in V_{max} but not the increase in K_{actin} (Fig. 4), suggesting that Ca^{2+} does not influence the interaction between myosin X and actin. It has been shown for myosin I and myosin V that 1–2 mol of calmodulin/mol of myosin head

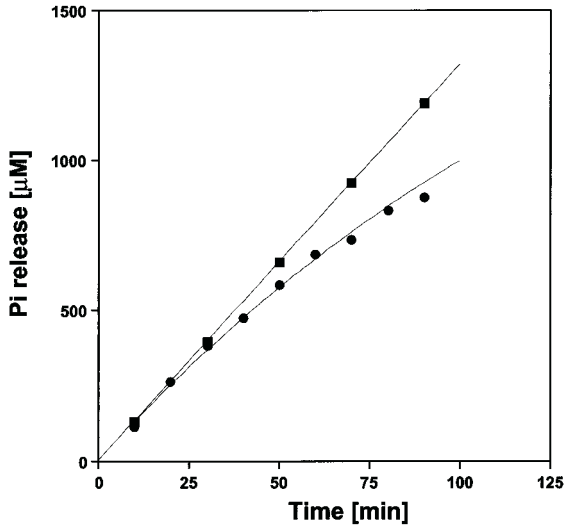

FIG. 5. **Time course of the actin-activated ATPase activity of M10CC with and without the ATP-regenerating system.** ATPase activity was measured in the presence (■) and absence ( ) of 20 units/ml pyruvate kinase and 3 mM phosphoenol pyruvate using 50 μM actin.

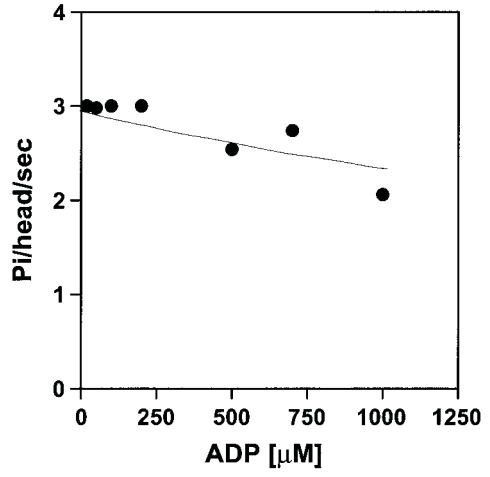

FIG. 6. **Inhibition of the actin-activated ATPase activity of M10CC by ADP.** The ATPase activity was measured as described in the legend for Fig. 5. A *solid line* is the calculated line based upon the equation $v = V_m[\mathrm{ATP}]/(K_{\mathrm{ATP}}(1 + [\mathrm{ADP}]/K_{\mathrm{ADP}}) + [\mathrm{ATP}])$. According to the analysis, a K_{ADP} of 6.4 μM was obtained.

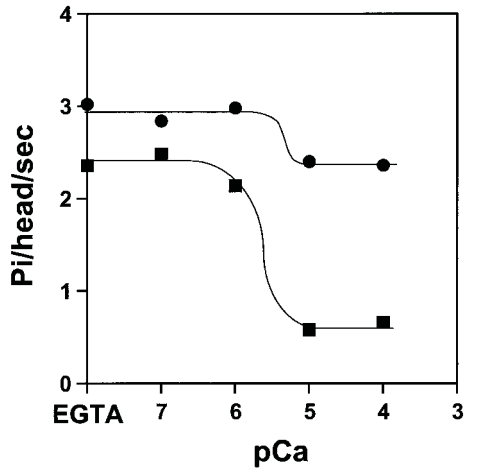

FIG. 7. **Effects of Ca^{2+} on the actin-activated ATPase activity of M10CC.** Actin-activated ATPase activity of M10CC (52 nM) was assayed in buffer containing 50 μM actin, 20 mM MOPS (pH 7.0), 10 mM KCl, 2 mM $MgCl_2$, 2 mM ATP, and 1 mM $CaCl_2$ with various concentrations of EGTA at 25 °C. Exogenous calmodulin (200 μg/ml) was added where indicated. , with calmodulin; ■, without calmodulin.

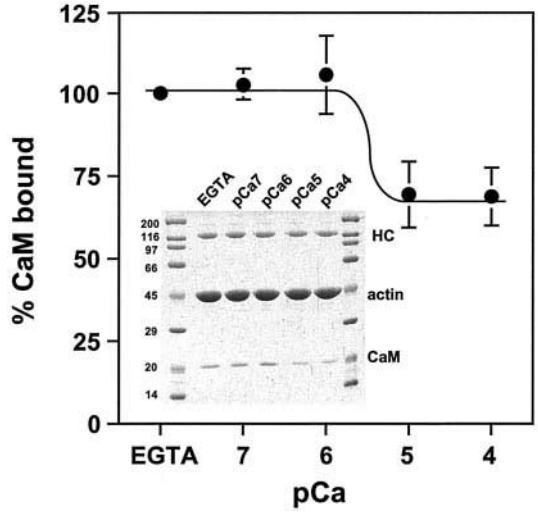

FIG. 8. **Effects of Ca^{2+} on the dissociation of calmodulin from M10CC.** M10CC (5 μg/ml) was dialyzed against buffers of *p*Ca 7, 6, 5, and 4 and then actin (0.025 mg/ml) was added. After centrifugation (100,000 × *g*, 30 min), pellets were subjected to SDS-polyacrylamide gel electrophoresis, and the concentrations of M10CC and calmodulin were determined by densitometry. The experiment was done three times, and the *bars* represent standard deviation. The *inset* shows SDS-PAGE of the pellets of M10CC co-precipitated with actin. *CaM*, calmodulin; *HC*, heavy chain.

dissociates from the heavy chain at high Ca^{2+}, and this is attributed to the change in the ATPase activity. Therefore, we examined whether the bound calmodulin of myosin X dissociates from the heavy chain at high Ca^{2+}. M10CC was mixed with F-actin in various free Ca^{2+} concentrations and then ultracentrifuged to determine the amount of bound calmodulin to myosin X. The myosin X-bound calmodulin co-precipitated with actin was analyzed by SDS-PAGE, and the amount of calmodulin was quantitated by densitometry with normalization with myosin X heavy chain. As a control, free calmodulin was centrifuged with F-actin, but no calmodulin co-precipitation was detected. M10CC was not precipitated at all in the absence of F-actin (not shown). As shown in Fig. 8, the amount of calmodulin bound to M10CC decreased at Ca^{2+} concentrations above *p*Ca 5. The densitometric analysis revealed that 1 mol of the bound calmodulin dissociates from the myosin X heavy chain.

In Vitro Motility Activity of Myosin X—Fig. 9 shows the motility activity of M10CC at various calcium ion concentrations. The velocity was 0.3 μm/s under 1 mM EGTA conditions, but the motility activity was completely inhibited at Ca^{2+} concentrations higher than *p*Ca 6. The inhibition of the motility was not rescued by the addition of exogenous calmodulin (up to 60 μM) (Fig. 9*B*), suggesting that the inhibition of the motility is not due to the dissociation of calmodulin from myosin X but rather due to the conformational change of the bound calmodulin upon Ca^{2+} binding. Consistently no detectable calmodulin dissociation was observed at *p*Ca 6 (Fig. 8). The motility inhibited at *p*Ca 6 was recovered by reducing the Ca^{2+} concentration to *p*Ca 7 without the addition of exogenous calmodulin.

Fig. 10 shows the actin sliding velocity of the *in vitro* motility assay as a function of ATP concentration. M10CC moved the actin filaments at low ATP concentration and reached the maximum velocity at 100 μM ATP. The low ATP requirement of the motility activity is also found for myosin II and myosin V and is consistent with the low K_{ATP} value for the actin-activated ATPase activity of myosin X.

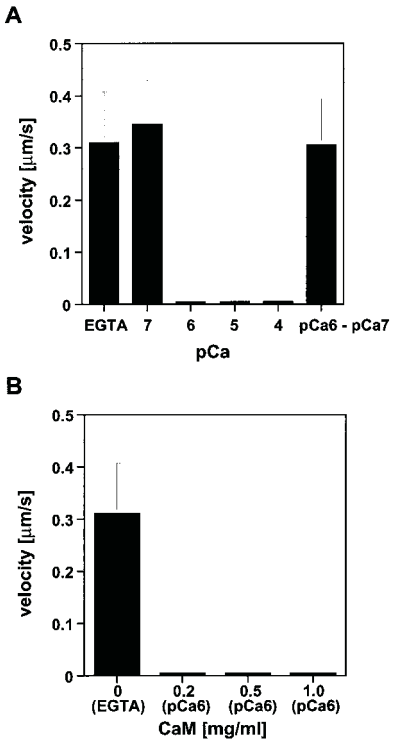

FIG. 9. **Ca^{2+} and calmodulin dependence of the actin filament sliding velocity of M10CC.** *A*, effect of Ca^{2+} on the actin filament sliding velocity. Actin filament motility was observed in 20 mM MOPS (pH 7.0), 10 mM KCl, 5 mM $MgCl_2$, 1 mM dithiothreitol, 4.5 mg/ml glucose, 216 μg/ml glucose oxidase, 36 μg/ml catalase, 0.5% methylcellulose, and 5 mM ATP at 25 °C. *pCa 6-pCa 7*, M10CC was first applied into the flow cell at *p*Ca 6 and then the flow cell was reperfused with *p*Ca 7 buffer. The *bars* represent the standard deviation with 10–20 actin filaments observed for motility assay. *B*, exogenous calmodulin (*CaM*) fails to rescue the inhibition of the motility at high Ca^{2+}.

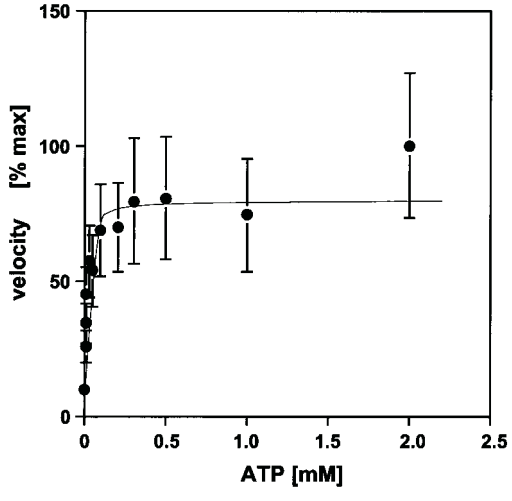

FIG. 10. **The actin filament sliding velocity of M10CC as a function of ATP concentration.** Actin filament motility was observed as described in the legend for Fig. 9, except various ATP concentrations and an ATP regeneration system (20 units/ml pyruvate kinase and 3 mM phosphoenol pyruvate) were used in the EGTA condition. The *bars* represents the standard deviation with 10–20 actin filaments observed for motility assay.

Direction of the Movement—Quite recently it was shown that the mammalian class VI myosin is a minus end-directed motor in contrast to other known myosins (11). Myosin VI has a unique insertion between the motor domain and the neck domain, and this was hypothesized to be responsible for the reverse directionality of motility (11). However, recent finding

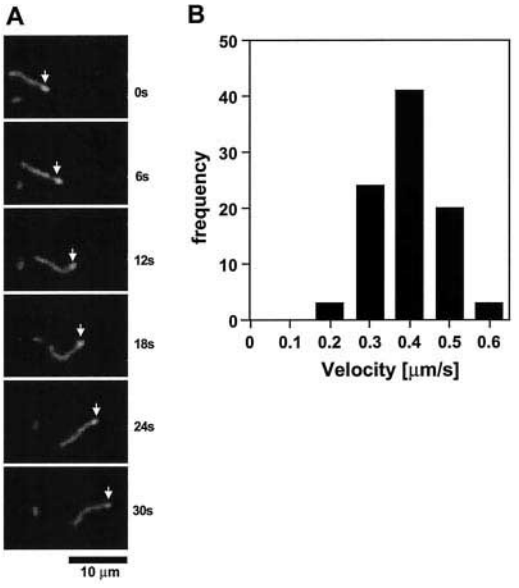

FIG. 11. **Direction of the movement of M10CC.** *A*, movement of the dual labeled F-actin on an M10CC-coated coverslip. Times are indicated on the *right* of panel. Data were obtained with a conventional *in vitro* motility assay with dual fluorescent-labeled F-actin. The *bright tip* on the actin filament represents the minus end of the filament. The *white arrows* in *A* indicate the leading part of the dual labeled actin filaments at the front. The pointed end of the actin filaments led the movement, indicating that M10CC moves toward the barbed end of F-actin. *B*, histogram of the velocities of actin filaments having polarity markers. Movement toward the barbed end of F-actin is defined as a positive value.

questioned this view (12), opening up the possible presence of other minus end-directed myosin motors within the myosin superfamily. We used dual fluorescent-labeled F-actin filaments in the *in vitro* motility assay to determine the direction of movement of myosin X. F-actin was labeled throughout with fluorescein and labeled with a tetramethylrhodamine cap at the pointed end of the filament.

The dual fluorescent-labeled F-actin filaments were visualized under the fluorescence microscope moving on coverslips coated with myosin X. As shown in Fig. 11*A*, myosin X moved the dual fluorescence-labeled F-actin with the pointed end at the front of the movement. This means that myosin X moves toward the barbed end as is known for the conventional myosins. Fig. 11*B* shows a histogram of the velocities of polarity-marked actin filaments on myosin X-coated coverslips. Although some variation of the sliding velocity was observed, all actin filaments moved in the same direction. The result shows that myosin X is a plus-directed motor.

Binding of Myosin X to Actin—It is known that myosin dissociates upon ATP binding to produce a weak actin binding form. The binding of myosin X to actin in the presence of ATP was measured by actin co-sedimentation assay. Myosin X was readily dissociated from actin in the presence of ATP, and a predominant amount of myosin X was recovered in the supernatant (Fig. 12). This property is similar to conventional myosin but different from myosin V. The result is consistent with the high K_{actin} of the actomyosin X ATPase reaction and suggests that the predominant intermediate of the myosin X ATPase reaction is a weak actin binding form.

Actin Filament Velocity as a Function of Myosin Density—It is known that actin filaments detach from the coverslip surface below a certain critical surface density of the nonprocessive motors, whereas a processive motor binds and holds an actin filament even at a low surface density. This is closely related to the difference in the duty ratio of the two types of motors. Fig. 13 shows the actin filament velocity as a function of various

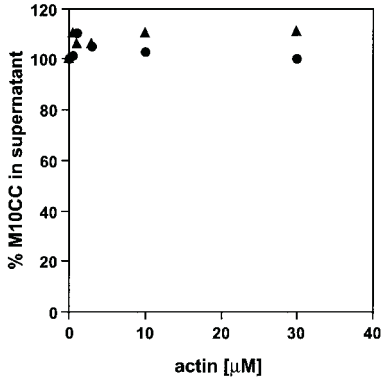

FIG. 12. **Dissociation of acto-M10CC by ATP.** The co-sedimentation assay was performed as follows. M10CC was incubated in buffer containing 20 mM MOPS (pH 7.0), 10 mM KCl, 5 mM $MgCl_2$, 2 mM ATP, and various concentrations of F-actin in the presence of an ATP regeneration system (20 units/ml pyruvate kinase and 3 mM phosphoenol pyruvate) at 25 °C for 10 min. The samples were ultracentrifuged at 100,000 × *g* for 30 min, and the supernatants were analyzed by SDS-polyacrylamide gel electrophoresis. The amount of the M10CC heavy chain in the supernatant was determined by densitometry as described previously (13). , 1 mM EGTA; ▲, *p*Ca 4.

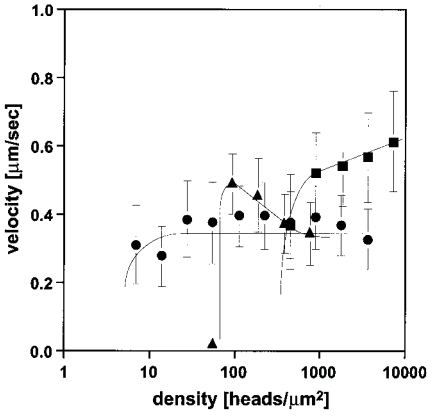

FIG. 13. **Actin filament velocity as a function of myosin surface density.** The surface density was calculated by the myosin concentration times the flow cell volume divided by the area of both flow cell faces assuming all the myosins added were attached on the glass surface. This would provide a high end of the molecules per unit area. , myosin V heavy meromyosin; ■, smooth muscle phosphorylated myosin II; ▲, M10CC.

myosin surface densities. The actin filament velocity over myosin V did not change over a wide range of surface densities and supported the motility at very low surface density. On the other hand, smooth muscle myosin II dropped in velocity as the density decreased. Myosin X motility also dropped with decreasing surface density, but the critical density was significantly lower than that for smooth muscle myosin II. Because the surface density dependence of the motility velocity is closely related to the duty ratio of the motors (31), the result suggests that the duty ratio of myosin X is higher than that of myosin II, although its duty ratio would not be as sufficiently high as a processive motor.

DISCUSSION

Myosin X is a newly found member of the myosin superfamily that is composed of at least 18 classes (1–6). Quite recently it was reported that myosin X in cultured cells is present at the edge of lamellipodia, membrane ruffles, and tips of filopodial actin bundles, suggesting that myosin X plays a role where actin structure dynamically changes (7). This finding as well as the primary structure of myosin X has led to the suggestion that it may be a motor protein, yet there is no information about the motor function of myosin X and its regulation at a molecular level. The present study revealed for the first time the mechanoenzymatic characteristic of myosin X and its regulation at a molecular level.

One of the critical issues to understand the physiological function of various types of myosins is the motor characteristic of each type of myosin. For instance, a processive motor that proceeds many steps without dissociating from actin is suitable for supporting cargo movements, whereas a nonprocessive motor is preferable for fast movement or high force production because many motor molecules can interact with a single actin filament without interfering with each other. The present results indicate that myosin X has a weak affinity for actin in the presence of ATP because 1) a majority of myosin X dissociated from actin in the presence of ATP and 2) K_{actin} for the actin-activated ATPase activity is high. The results also suggest that the predominant steady state intermediate of actomyosin X ATPase is a weak actin binding state. This is different from myosin V, a processive myosin, which shows a strong actin binding in the presence of ATP. This is because M·ADP (where M refers to a myosin head), a strong actin binding intermediate, is the predominant reaction intermediate of the ATPase reaction (28) and rather similar to myosin II, a nonprocessive myosin. Consistently the actomyosin X ATPase activity was hardly inhibited by ADP suggesting that the ADP release step is not rate-limiting for the ATPase reaction. This is in contrast to the myosin V ATPase reaction where ADP markedly inhibits the steady state actin-activated ATPase activity (28). These results indicate that myosin X is a nonprocessive myosin. To further address this issue, we examined the actin translocating velocity as a function of myosin X surface density in the *in vitro* gliding actin filament assay. It was revealed that myosin X can support the actin filament movement at a significantly lower surface density than myosin II but at a surface density much higher than that of myosin V. The result suggests that although myosin X is a nonprocessive myosin, its duty ratio would be significantly larger than that of myosin II.

Another important issue of the motor characteristic of myosin is the directionality. The recent finding of myosin VI to step in a backward direction fundamentally changed the view of polarity of actin filament-based movements in cells. According to Wells *et al.* (11), a large insertion between the motor domain and IQ domain present in myosin VI is a determinant of the reverse directionality of myosin VI. However, this view was questioned recently (12) raising the possibility of other unconventional myosins having reverse directionality. Therefore, we examined the directionality of myosin X using dual fluorescent-labeled F-actin filaments. The present result clearly demonstrated that myosin X is a plus-directed myosin unlike myosin VI. No actin filaments moved to the opposite direction indicating that the directionality is uniquely determined with myosin motor without any fluctuation of the biased movement.

Ca^{2+} dependence of the actin-activated ATPase activity showed a sharp decrease in the activity above *p*Ca 6. This decrease in the activity is due to the dissociation of 1 mol of calmodulin light chain because 1) the decrease in the activity is rescued by the addition of exogenous calmodulin and 2) 1 mol of calmodulin light chain dissociated from myosin X heavy chain at *p*Ca 5 and higher. Similar findings have been made with myosin V (18). On the other hand, the actin translocating activity of myosin X is inhibited at *p*Ca 6 in which no significant dissociation of calmodulin occurs. The inhibition of the motility of calmodulin-containing mammalian unconventional myosins was first demonstrated with myosin I (13–17) and then subsequently with myosin V (18, 30). It was thought originally that the inhibition of the motility is due to the dis-

sociation of calmodulin from the heavy chain at high Ca^{2+} (15). But recent studies have revealed that the inhibition does not require the dissociation of calmodulin but that Ca^{2+} binding at the high affinity sites of calmodulin triggers the inhibition presumably because of a large conformational change of calmodulin (13, 14, 18). Addition of exogenous calmodulin did not rescue the inhibition of the motility activity of myosin X unless Ca^{2+} concentration was decreased. These results are consistent with the recent results with myosin V and myosin Iβ and indicate that the dissociation of calmodulin is not directly related to the inhibition of motility, but the conformational change of the heavy chain-bound calmodulin upon binding of Ca^{2+} is responsible for the inhibition of the movement. The inhibition occurs between *p*Ca 7 and *p*Ca 6 at which cytoplasmic Ca^{2+} concentration is regulated in most cell types, and therefore the observed inhibition is physiologically relevant.

There is an apparent decoupling between the ATP hydrolysis cycle and mechanical events at higher Ca^{2+}. This is different from the regulation of conventional myosins in which the regulatory domain regulates both ATPase and mechanical activities (32–34). The mechanism that underlies the apparent uncoupling between the ATP hydrolysis and the motility is unknown. One possibility is that a change in the rigidity at the lever-arm domain of myosin upon Ca^{2+} binding to calmodulin could uncouple the mechanical activity and ATP hydrolysis of myosin. Further studies are required to clarify the mechanism underlying the uncoupling of ATP hydrolysis and motility.

While this manuscript was in preparation, Chen *et al.* (35) reported in abstract form that mammalian myosin X has an actin-activated ATPase activity with a V_m of 10 s^{-1} at 37 °C and an actin translocating velocity of 0.18 μm/s at 30 °C. The values for the ATPase activity are comparable with the present study (V_m of 4.7 s^{-1} at 25 °C), but the actin sliding velocity is lower than that of the present study (0.3 μm/s at 25 °C). Quite recently it was reported that calmodulin-like protein (CLP) can serve as a light chain of myosin X in epithelial cells (36). However, CLP is only expressed in epithelial cells, whereas myosin X is expressed in a variety of tissues (7) that do not express CLP. Therefore, it is likely that calmodulin rather than CLP is the light chain of myosin X in most tissues. It should be noted that it was reported that myosin X shows higher affinity for calmodulin than for CLP and that the actin-activated ATPase activity of myosin X is not markedly affected by the difference in the light chains, *i.e.* calmodulin or CLP (35). Further study is required for the function of CLP in myosin X motor properties.

Acknowledgment—We thank Dr. D. P. Corey (Harvard University) for providing us myosin X cDNA fragments.

REFERENCES

1. Mooseker, M. S., and Cheney, R. E. (1995) *Annu. Rev. Cell Dev. Biol.* **11,** 633–675
2. Titus, M. A. (1997) *Trends Cell Biol.* **7,** 119–123
3. Hodge, T., and Cope, M. J. (2000) *J. Cell Sci.* **113,** 3353–3354
4. Sellers, J. R. (1999) *Myosins*, 2nd Ed., Oxford University Press, Oxford
5. Kellerman, K. A., and Miller, K. G. (1992) *J. Cell Biol.* **119,** 823–834
6. Baker, J. P., and Titus, M. A. (1997) *J. Mol. Biol.* **272,** 523–535
7. Berg, J. S., Derfler, B. H., Pennisi, C. M., Corey, D. P., and Cheney, R. E. (2000) *J. Cell Sci.* **113,** 3439–3451
8. Yonezawa, S., Kimura, A., Koshiba, S., Masaki, S., Ono, T., Hanai, A., Sonta, S., Kageyama, T., Takahashi, T., and Moriyama, A. (2000) *Biochem. Biophys. Res. Commun.* **271,** 526–533
9. Mehta, A. D., Rock, R. S., Rief, M., Spudich, J. A., Mooseker, M. S., and Cheney, R. E. (1999) *Nature* **400,** 590–593
10. Walker, M. L., Burgess, S. A., Sellers, J. R., Wang, F., Hammer, J. A., III, Trinick, J., and Knight, P. J. (2000) *Nature* **405,** 804–807
11. Wells, A. L., Lin, A. W., Chen, L. Q., Safer, D., Cain, S. M., Hasson, T., Carragher, B. O., Milligan, R. A., and Sweeney, H. L. (1999) *Nature* **401,** 505–508
12. Homma, K., Yoshimura, M., Saito, J., Ikebe, R., and Ikebe, M. (2001) *Biophys. J.* **80,** 573a
13. Zhu, T., Sata, M., and Ikebe, M. (1996) *Biochemistry* **35,** 513–522
14. Zhu, T., Beckingham, K., and Ikebe, M. (1998) *J. Biol. Chem.* **273,** 20481–20486
15. Collins, K., Sellers, J. R., and Matsudaira, P. (1990) *J. Cell Biol.* **110,** 1137–1147
16. Swanljung-Colling, H., and Colling, J. H. (1991) *J. Biol. Chem.* **266,** 1312–1319
17. Barylko, B., Wagner, M. C., Reizes, O., and Albanesi, J. P. (1992) *Proc. Natl. Acad. Sci. U. S. A.* **90,** 490–494
18. Homma, K., Saito, J., Ikebe, R., and Ikebe, M. (2000) *J. Biol. Chem.* **275,** 34766–34771
19. Spudich, J. A., and Watt, J. (1971) *J. Biol. Chem.* **246,** 4866–4871
20. Chien, Y. H., and Dawid, I. B. (1984) *Mol. Cell. Biol.* **4,** 507–513
21. Ikebe, M., Kambara, T., Stafford, W. F., Sata, M., Katayama, E., and Ikebe, R. (1998) *J. Biol. Chem.* **273,** 17702–17707
22. Ikebe, M., and Hartshorne, D. J. (1985) *J. Biol. Chem.* **260,** 13146–13153
23. Ikebe, M., Stepinska, M., Kemp, B. E., Means, A. R., and Hartshorne, D. J. (1989) *J. Biol. Chem.* **264,** 6967–6971
24. Laemmli, U. K. (1970) *Nature* **227,** 680–685
25. Reynard, A. M., Hass, L. E., Jacobsen, D. D., and Boyer, P. D. (1961) *J. Biol. Chem.* **236,** 2277–2282
26. Sata, M., Matsuura, M., and Ikebe, M. (1996) *Biochemistry* **35,** 11113–11118
27. Trybus, K. M., Kremensova, E., and Freyzon, Y. (1999) *J. Biol. Chem.* **274,** 27448–27456
28. DeLa Cruz, E. M., Wells, A. L., Rosenfeld, S. S., Ostap, E. M., and Sweeney, H. L. (1999) *Proc. Natl. Acad. Sci. U. S. A.* **96,** 13726–13731
29. Perreault-Micale, C., Shushan, A. D., and Coluccio, L. M. (2000) *J. Biol. Chem.* **275,** 21618–21623
30. Cheney, R. E., O'Shea, M. K., Heuser, J. E., Coelho, M. V., Wolenski, J. S., Espreafico, E. M., Forscher, P., Larson, R. E., and Mooseker, M. S. (1993) *Cell* **75,** 13–23
31. Rock, R. S., Rief, M., Mehta, A. D., and Spudich, J. A. (2000) *Methods* **22,** 373–381
32. Hartshorne, D. J. (1987) in *Physiology of the Gastrointestinal Tract* (Johnson, L. R., ed) 2nd Ed., Vol. 1, pp. 423–482, Raven Press, New York
33. Sellers, J. R., and Adelstein, R. S. (1987) in *The Enzymes* (Boyer, P., Krebs, and E. G., eds) Vol. 18, pp. 381–418, Academic Press, San Diego
34. Tan, J. L., Ravid, S., and Spudich, J. A. (1992) *Annu. Rev. Biochem.* **61,** 721–759
35. Chen, L., Wang, F., Meng, H., and Sellers, J. R. (2001) *Biophys. J.* **80,** 573a
36. Rogers, M. S., and Strehler, E. E. (2001) *J. Biol. Chem.* **276,** 12182–12189